

## ORIGINAL ARTICLE

# Alteration of Type I collagen microstructure induced by estrogen depletion can be prevented with drug treatment

Meagan A Cauble<sup>1</sup>, Edward Rothman<sup>2,3</sup>, Kathleen Welch<sup>3</sup>, Ming Fang<sup>1</sup>, Le T Duong<sup>4</sup>,  
Brenda L Pennypacker<sup>4</sup>, Bradford G Orr<sup>5</sup> and Mark M Banaszak Holl<sup>1,6</sup>

<sup>1</sup>Department of Chemistry, University of Michigan, Ann Arbor, MI, USA. <sup>2</sup>Department of Statistics, University of Michigan, Ann Arbor, MI, USA. <sup>3</sup>Center for Statistical Consultation and Research (CSCAR), University of Michigan, Ann Arbor, MI, USA. <sup>4</sup>Bone Biology Group, Merck Research Laboratories, West Point, PA, USA. <sup>5</sup>Department of Physics, University of Michigan, Ann Arbor, MI, USA. <sup>6</sup>Department of Biomedical Engineering, University of Michigan, Ann Arbor, MI, USA.

Two independent biological replicates of estrogen depletion were employed with differing drug treatment conditions. Data Set I consisted of 9-month-old New Zealand white female rabbits treated as follows: sham-operated ( $n = 11$ ), ovariectomized (OVX;  $n = 12$ ), OVX + 200  $\mu\text{g kg}^{-1}$  alendronate (ALN), 3  $\times$  a week for 27 weeks ( $n = 12$ ) and OVX + 10  $\text{mg kg}^{-1}$  Cathepsin-K inhibitor (CatKI) daily for 27 weeks. Data Set II consisted of 6-month-old New Zealand white female rabbits that were sham-operated ( $n = 12$ ), OVX ( $n = 12$ ) or OVX + 0.05  $\text{mg kg}^{-1}$  17 $\beta$ -estradiol (ERT) 3  $\times$  a week for 13 weeks ( $n = 12$ ). Samples from the cortical femur were polished and demineralized to make them suitable for atomic force microscopy (AFM) imaging. Type I collagen fibrils present in bundles or sheets, running parallel to each other, were combined into a class termed *Parallel*. Fibrils present outside of such structures, typically in images with an angular range of non-parallel fibrils, were combined into a class termed *Oblique*. The percentage of fibrils coded as *Parallel* for Sham animals in Data Sets I and II was 52% and 53%, respectively. The percentage of fibrils coded as *Parallel* for OVX animals in Data Sets I and II was 35% in both cases. ALN and ERT drug treatments reduced the change from 18 to 12%, whereas CatKI treatment reduced the change to 5%.

BoneKEy Reports 4, Article number: 697 (2015) | doi:10.1038/bonekey.2015.66

## Introduction

Reduction in estrogen level affects over 75 million people worldwide by inducing *Osteoporosis* and *Osteopenia*, decreasing overall bone quality and increasing susceptibility to fracture.<sup>1,2</sup> Clinical and scientific assessments have focused heavily on bone mineral density (BMD) as the primary assay of bone quality and drug treatment outcomes. However, BMD has demonstrated limitations for predicting bone fracture and understanding the roles of estrogen in bone quality, formation and resorption.<sup>3–5</sup> In particular, BMD is unable to assess changes in Type I collagen structure that are keys to understanding bone toughness. The structural changes that occur in Type I collagen matrix under conditions of estrogen depletion and drug treatment remain largely unknown. Here we show that the Type I collagen microstructure is altered by estrogen depletion and that this change is largely prevented by treatment with a Cathepsin-K inhibitor (CatKI) and partially prevented with

bisphosphonate or estradiol (ERT) treatment. These observations are particularly surprising for the bisphosphonate drug, which was developed to help maintain BMD and represents a new understanding of biochemical activity for this decade-old therapeutic. The ability of an inhibitor of the collagenase cathepsin-K to prevent estrogen-induced changes in Type I collagen microstructure is also previously unknown.

## Results

Changes in Type I collagen microstructure and nanomorphology are conveniently measured using atomic force microscopy (AFM).<sup>6,7</sup> Recent AFM studies indicated changes in the nanomorphology of the Type I collagen fibrils in ovariectomized (OVX) sheep<sup>8–10</sup> and rats.<sup>11</sup> In order to explore the effect of estrogen depletion and compare efficacy of CatKI and alendronate (ALN) drug treatments, the rabbit OVX model was developed by Merck Inc., as human CatKI's exhibit similar

Correspondence: Dr MM Banaszak Holl, Department of Chemistry, University of Michigan, 930 N. University Avenue, Ann Arbor, MI 48109-1055, USA.  
E-mail: mbanasza@umich.edu

Received 2 April 2014; accepted 12 December 2014; published online 27 May 2015

potency for the rabbit enzyme and the adult rabbit skeleton undergoes substantial cortical Haversian remodeling (unlike the rodent).<sup>12</sup> Nine-month-old New Zealand white female rabbits (Data Set I) underwent the following treatments: sham operation + vehicle ( $n = 11$ ), ovariectomy + vehicle (OVX;  $n = 12$ ), OVX + 200  $\mu\text{g kg}^{-1}$  ALN, 3  $\times$  a week for 27 weeks ( $n = 12$ ) and OVX + 10  $\text{mg kg}^{-1}$  CatKI L-235 daily for 27 weeks. Treatments were initiated 3 days after surgery. Data Set II consisted of 6-month-old New Zealand white female rabbits that underwent the following treatments: sham operation + vehicle ( $n = 12$ ), ovariectomy + vehicle (OVX;  $n = 12$ ) or OVX + 0.05  $\text{mg kg}^{-1}$  ERT 3  $\times$  a week for 13 weeks ( $n = 12$ ). Treatments were initiated 17 days after surgery. Both studies were performed in prevention mode with drug dosing initiated soon after surgery. Sample sets were stored in 95% ethanol. Rabbit cortical femur samples were polished for 90 s, followed by sonication for 5 min. Demineralization was carried out for 90 min (9-month old) or 120 min (6-month old) using 0.5 M EDTA at pH 8.0. The samples were sonicated for 5 min before imaging. We confirmed that ethanol fixation did not change the overall distribution of collagen fibril D-spacings or microstructure by direct comparison with the analysis of fresh, frozen rabbit bone. AFM images were obtained using tapping mode in air using silicon cantilevers (tip radius 10 nm, force constant 40  $\text{N m}^{-1}$  and resonance frequency 300 kHz). Details on sample preparation, imaging and image analysis protocols for Type I collagen in bone have been previously published.<sup>6</sup> Images were obtained from locations from across the full 1.00  $\times$  0.75 cm section of the femur mid-diaphysis (Supplementary Figure S1). All images were acquired in the plane parallel to the long bone axis and obtained from polished regions 100–300  $\mu\text{m}$  below the bone surface. No variation in the collagen structure was noted as a function of the polishing depth employed. Image acquisition for the mid-diaphysis sections proceeded using the following procedure. First, 30  $\times$  30- $\mu\text{m}$  scans were obtained in six regions of the 1.00  $\times$  0.75-cm bone imaging area. These were followed by 10  $\times$  10- $\mu\text{m}$  scans, and finally the 3.5  $\times$  3.5  $\mu\text{m}$  scans employed for image analysis. This approach ensured that the nano- to-micro-scale analysis of collagen fibrils was distributed across the 0.75  $\times$  1.0-cm imaging area. An average of six 30  $\times$  30- $\mu\text{m}$  scans and thirteen 3.5  $\times$  3.5- $\mu\text{m}$  scans were obtained per animal. From these regions, the average of 75 fibrils per animal was obtained. The local microstructure about each fibril was examined and coded as either *Parallel* or *Oblique*. In a given image area, it is thus possible for both *Parallel* and *Oblique* fibrils to be present. Furthermore, the assignment is indicative of a local order between fibrils with a length scale of a few hundred nanometers. The assessment does not provide evidence, one way or the other, of overall micron- to millimeter-scale order as typically measured using X-ray diffraction methods.

Exemplar images highlighting the features observed in the local structural organization of the fibrils are illustrated in **Figure 1**. We noted two major qualitative features in the images: (1) *Parallel* regions of fibrils with subclasses of bundles (3–15 fibrils aligned in parallel with defined edges) and sheets (>20 fibrils aligned in a planar, parallel manner); (2) *Oblique* regions of fibrils exhibiting an angular range of fibril orientation. For all samples, the nanomorphology of individual fibrils, as quantified using the metric of the D-spacing, was measured, and each fibril was coded (blinded of the sample origin) for its

local microstructure. Fibrils coded as present in bundles or sheets (**Figure 1a**) were grouped together as *Parallel* regions. A number of other features were also coded including fibril pairs and individual fibrils crossing bundles or sheets (Supplementary Figure S2). Roughly half of the fibrils observed were present in structures without the same degree of parallel alignment, exhibited a wide range of fiber–fiber angular dispersion and were classified as being present in the *Oblique* regions (**Figure 1b**). A total of 5673 individual fibrils were classified from 1081 3.5  $\times$  3.5- $\mu\text{m}$  images from a total of 94 animals across the seven experimental groups. The coding and frequency of *Parallel* and *Oblique* observations are summarized in **Table 1**. In all cases, the *Parallel* and *Oblique* codings captured  $\geq 95\%$  of all measured fibrils. Additional exemplar images for the Sham, OVX, ALN, CatKI and ERT treatments are provided in Supplementary Figure S4.

To assess the significance of the differences in proportion of fibrils that are in *Parallel* and *Oblique* regions by the treatment group, we employed a logistic regression model using generalized estimating equations (GEEs),<sup>13</sup> with correlations between any two pairs of observations within the same animal being constant, estimated from the data. The proportion of each type of fibril was compared for each treatment versus sham using a binary outcome,  $Y_{ij}$ , where  $Y_{ij} = 1$  if the fibril was in a given microenvironment (that is, *Parallel* or *Oblique*) and  $Y_{ij} = 0$  if the fibril was not, with a logit link function. All s.e.'s were computed using the robust Huber–White estimates. The GEE model that was employed is shown below:

$$\text{logit}(p_{ij}) = \log\left(\frac{p_{ij}}{1-p_{ij}}\right) = \beta_0 + \sum_{t=1}^{T-1} \beta_t \text{Treatment}_t$$

where  $p_{ij}$  = probability ( $Y_{ij} = 1$ ) for fibril  $i$  in animal  $j$ ,  $\beta_0$  is the intercept and  $\beta_t$  fits the effect of treatment  $t$ ,  $t = 1$  to  $T$ , with treatment  $T$  being the reference category.

*Post hoc* comparisons of collagen fibril orientations were then carried out between treatment groups, using a Bonferroni correction for multiple comparisons with statistical significance assigned for  $P$ -values below 0.05.

Compared with Sham, the OVX-treated animals in Data Set I had a 17% decrease ( $P$ -value = 0.0045) in the proportion of fibrils occurring in *Parallel* structures and an 18% increase ( $P$ -value = 0.0026) in the proportion of fibrils occurring in *Oblique* structures. ALN treatment was previously observed to function as an antiresorptive leading to a BMD higher than that in the vehicle-treated group.<sup>12</sup> In this study, ALN treatment resulted in a frequency of collagen fibril observations intermediate between Sham and OVX values, although the differences in proportions of fibrils in *Parallel* and *Oblique* regions in these treatments were not significant. The bone resorption inhibitor CatKI also gave intermediate values for the frequency of collagen fibril observations and showed even less shift from the initial Sham values, with none of the comparisons versus other treatments being significant. Statistically, the changes in the proportion of fibrils in *Parallel* and *Oblique* regions for the drug-treated sample were not significantly different from the Sham samples. *These data indicate that the drugs prevent the OVX-induced change in the collagen microstructure in addition to their traditionally understood roles of preventing decreases in BMD.* For the OVX treatment in Data Set II, an 18% decrease ( $P$ -value = 0.0188) was observed in the proportion of fibril

occurrence in *Parallel* structures and a 20% increase ( $P$ -value = 0.0048) was observed in the proportion of fibril occurrence in *Oblique* structures compared with Sham. ERT treatment resulted in a partial prevention of change in the collagen microstructure, although the difference in ERT versus Sham in proportion of *Parallel* region fibrils was not significant ( $P = 0.0961$ ), whereas the difference in the proportion of *Oblique* fibrils was significant (0.0185). The magnitude of observed changes was similar to ALN treatment and less effective compared with CatKI treatment in preventing microstructure change. Analysis of the D-spacing variation for all seven samples showed a range of values between ~58 and 70 nm, consistent with previous observations of D-spacing distribution.<sup>6,8,14</sup> However, no shift of the D-spacing values was observed for these samples, unlike the previous comparison for Sham and OVX sheep samples (Supplementary Figure S3).<sup>8,9</sup>

### Discussion

OVX is a common model used to study the effects of estrogen depletion.<sup>8,9,15-17</sup> Pennypacker *et al.*<sup>12</sup> applied the OVX model to study osteopenia in rabbits using the samples described herein and demonstrated osteoclastic bone resorption resulting from estrogen depletion. On the basis of the strong positive correlations between the experimental strength parameters and the tissue bone mineral content from animals from the same study, it was demonstrated that there were no obvious treatment-related changes in the material properties of vertebrae and femurs in the OVX rabbits treated with odanacatib or

ALN for 27 weeks. Here, we directly examined the effects of estrogen deficiency and two different bone resorption inhibitors at the microfibril structure level and observed changes in the relative frequency of fibril occurrence in local *Parallel* and *Oblique* microstructures. The link between increased resorption and the changes reported here to Type I collagen fibril microstructure remains unknown; however, related studies in the literature provide clues to possible mechanisms. In the mouse model, OVX reduces proteoglycan levels.<sup>11</sup> Furthermore, biglycan and decorin knockout mice have abnormal collagen fibril morphologies.<sup>12</sup> We hypothesize that reduced proteoglycan levels perturb the interactions between adjacent fibrils, resulting in a change to the microstructure. Cathepsin-K, a collagenase secreted by osteoclasts, cleaves proteoglycans from the fibril exterior before degrading the primary fibril structure.<sup>18</sup> OVX results in increased osteoclast activity coupled to increased cathepsin-K activity. This is directly countered by the ERT therapy resulting in partial prevention of the collagen fibril microstructure changes. Strikingly, application of CatKI, which can prevent proteoglycan cleavage directly at the level of enzyme activity, gives almost complete prevention of fibril microstructure change. By way of contrast, treatment with a bisphosphonate is known to induce a change to osteoclast cell morphology and eventual cell death.<sup>19</sup> Thus, ALN reduces the amount of bone resorption, but also indirectly lowers the activity of cathepsin-K enzyme, which is consistent with observation that ALN treatment partially prevents changes to Type I collagen microstructure. Recently, Reznikov *et al.*<sup>20</sup> reported that the human lamellar bone consists of two different materials that differ substantially in terms of collagen fibril order. The connection between our fibril-level local organization classification (*Parallel* versus *Oblique*) and their observation of ‘ordered’ and ‘disordered’ materials is not clear at this time; however, changes in the relative quantities of the ‘ordered’ and the ‘disordered’ materials as a function of estrogen depletion and drug treatment are also a possible explanation of our data. These changes could also be related to the impacts of proteoglycan levels as discussed above.

In summary, a quantitative analysis of Type I collagen fibril organization indicates a significant decrease in fibrils appearing in *Parallel* structures such as bundles and sheets (18%) and a concomitant increase in fibrils appearing in *Oblique* structures, on OVX treatment of 6- and 9-month-old rabbits. ALN and ERT drug treatments partially prevent the microstructure changes (12% decrease in *Parallel* structures), and CatKI treatment

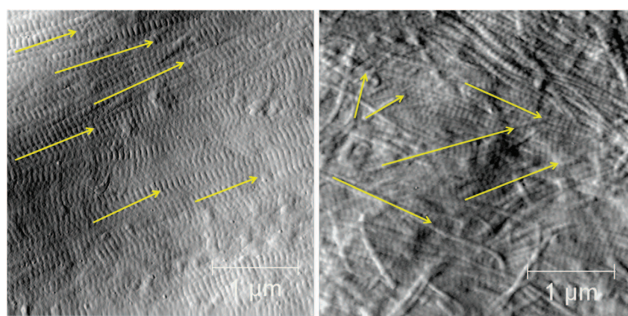


**Figure 1** AFM images illustrating *Parallel* and *Oblique* regions of Type I collagen fibrils. (a) *Parallel* region showing multiple aligned fibrils (yellow arrows); (b) *oblique* region showing multiple fibrils with varying alignment (yellow arrows).  $3.5 \times 3.5 \mu\text{m}$  image.

**Table 1** Frequency of Type I collagen fibrils observed in *Parallel* and *Oblique* microstructures

Treatment	No. of fibrils	No. of animals	Frequency in parallel microstructures (% , s.e.)	Frequency in oblique microstructures (% , s.e.)	Microstructure Frequency difference
<i>Data Set I</i>					
Sham	825	11	52 (5)	45 (5)	7(10)
OVX	808	12	35 (5)	63 (5)	- 28 (10)
ALN	971	12	40 (5)	57 (5)	- 17 (10)
CatKI	1001	13	47 (5)	49 (5)	- 2 (10)
<i>Data Set II</i>					
Sham	579	12	53 (5)	42 (5)	11 (10)
OVX	728	12	35 (5)	62 (5)	- 27 (10)
ERT	761	12	41 (4)	58 (4)	- 17 (10)

Abbreviations: ALN, alendronate; CatKI, Cathepsin-K inhibitor; ERT, estradiol; OVX, ovariectomized.

almost completely prevents the structural change (5% decrease in *Parallel* structures). The change in Type I collagen microstructure induced by OVX is a previously unrecognized aspect of the impact of estrogen depletion on bone quality. In addition, the amelioration of these microstructure changes is a previously unrecognized mechanism of drug activity.

### Materials and Methods

All rabbit femur samples were obtained from Merck Research Laboratory, West Point, PA, USA, and treatment of these animals was previously described in detail.<sup>12</sup> Sample preparation and the AFM imaging methods employed in this work have also been described in detail.<sup>6</sup> All imaging was carried out in air using a PicoPlus 5500 AFM (Agilent, Santa Clara, CA, USA) employing tapping mode with VistaProbes T300R probes (NanoScience, Phoenix, AZ, USA; nominal radius 10 nm, force constant 40 N m<sup>-1</sup>, resonance frequency 300 kHz). Line scan rates were set at 2 Hz or lower at 512 lines per frame. Image analysis and measurements were performed using the SPIP software (Image Metrology, Horsholm, Denmark).

### Conflict of Interest

LTD and BLP work for Merck Inc. The remaining authors declare no conflict of interest.

### Acknowledgements

This work was supported in part by an IISP grant from Merck Inc. to MMBH. We thank MD Morris and CM Les for many fruitful discussions on the impact of estrogen depletion and bisphosphonate treatment on bone. We thank HG Bone for fruitful discussions including suggesting the CatKI experiment, bringing to the attention of the UM group the unpublished Sham, OVX, CatKI, ALN and ERT studies of Pennypacker *et al.*<sup>12</sup> and introducing the UM group to the Bone Biology group at Merck Inc.

### References

1. Johnell O, Kanis JA. An estimate of the worldwide prevalence and disability associated with osteoporotic fractures. *Osteoporos Int* 2006; **17**: 1726–1733.
2. Viguet-Carrin S, Garnero P, Delmas PD. The role of collagen in bone strength. *Osteoporos Int* 2006; **17**: 319–336.
3. Burr DB. The contribution of the organic matrix to bone's material properties. *Bone* 2002; **31**: 8–11.
4. Cranney A, Guyatt G, Griffith L, Wells G, Tugwell P, Rosen C *et al.* Summary of meta-analyses of therapies for postmenopausal osteoporosis. *Endocr Rev* 2002; **23**: 570–578.
5. Sornay-Rendu E, Delmas PD. Advances in osteoporosis diagnosis: the use of clinical risk factors. *Mediographica* 2008; **30**: 350–554.
6. Erickson B, Fang M, Wallace JM, Orr BG, Les CM, Banaszak Holl MM. Nanoscale structure of type I collagen fibrils: quantitative measurement of D-spacing. *Biotechnol J* 2013; **8**: 117–126.
7. Fang M, Goldstein EL, Turner AS, Les CM, Orr BG, Fisher GJ *et al.* Type I collagen D-spacing in fibril bundles of dermis, tendon, and bone: bridging between nano- and micro-level tissue hierarchy. *ACS Nano* 2012; **6**: 9503–9514.
8. Wallace JM, Erickson B, Les CM, Orr BG, Banaszak Holl MM. Distribution of type I collagen morphologies in bone: relation to estrogen depletion in bone. *Bone* 2010; **46**: 1349–1354.
9. Fang M, Liroff KG, Turner AS, Les CM, Orr BG, Banaszak Holl MM. Estrogen depletion results in nanoscale morphology changes in dermal collagen. *J Invest Dermatol* 2012; **132**: 1791–1797.
10. Fang M, Banaszak Holl MM. Variation in type I collagen fibril nanomorphology: the significance and origin. *BoneKey* 2013; **2**: 394.
11. Kafantari H, Kounadi E, Fatourous M, Milonakis M, Tzaphlidou M. Structural alterations in rat skin and bone collagen fibrils induced by ovariectomy. *Bone* 2000; **26**: 349–353.
12. Pennypacker BL, Duong LT, Cusick TE, Masarachia PJ, Gentile MA, Gauthier JY *et al.* Cathepsin K inhibitors prevent bone loss in estrogen-deficient rabbits. *J Bone Miner Res* 2011; **26**: 252–262.
13. Diggle PJ, Heagerty P, Liang K-Y, Zeger SL. *Analysis of Longitudinal Data*. Oxford University Press, 2002.
14. Wallace JM, Chen Q, Fang M, Erickson B, Orr BG, Banaszak Holl MM. Type I collagen exists as a distribution of nanoscale morphologies in teeth, bones, and tendons. *Langmuir* 2010; **26**: 7349–7354.
15. Frost HM, Jee WSS. On the rat model of human osteopenias and osteoporosis. *Bone Miner* 1992; **18**: 227–236.
16. Kalu DN. The ovariectomized rat model of postmenopausal bone loss. *Bone Miner* 1991; **15**: 175–191.
17. Smith SY, Jollette J, Turner CH. Skeletal health: primate model of postmenopausal osteoporosis. *Am J Primatol* 2009; **71**: 752–765.
18. Panwar P, Du X, Sharma V, Lamour G, Castro M, Li HB *et al.* Effects of cysteine proteases on the structural and mechanical properties of collagen fibers. *J Biol Chem* 2013; **288**: 5940–5950.
19. Rogers MJ, Crockett JC, Coxon FP, Monkkonen J. Biochemical and molecular mechanisms of action of bisphosphonates. *Bone* 2011; **49**: 34–41.
20. Reznikov N, Shahar R, Weiner S. Three-dimensional structure of human lamellar bone: the presence of two different materials and new insights into the hierarchical organization. *Bone* 2014; **59**: 93–104.

Supplementary Information accompanies the paper on the BoneKey website (<http://www.nature.com/bonekey>).